

# Filtering the Continuous Wavelet Transform Using Hyperbolic Triangulations

Günther Koliander, Luis Daniel Abreu, Antti Haimi, and José Luis Romero

**Abstract**—We propose a methodology that detects signal components of a signal in white noise based on a hyperbolic triangulation of its wavelet transform (WT). The theoretical background is a connection between analyticity inducing wavelets and Gaussian analytic functions. This relation allows us to obtain some useful details on the random distribution of the zeros of the wavelet transformed signal. We apply our method to some acoustic signals and observe that many signal components are found but as predicted by the theory there is no guarantee to find all signal components.

**Index Terms**—Wavelet transform, hyperbolic geometry, Gaussian analytic functions

## I. INTRODUCTION

Identifying important components of signals embedded in a noisy background is a fundamental problem in signal analysis. A prevalent viewpoint is that these important components correspond to high-energy regions in some transform domain. Existing methods that conform to this viewpoint include (block-)thresholding methods [1], [2], “synchrosqueezing” [3] and “reassignment” [4], [5] methods, or methods based on ridges [6], [7]). A recently proposed complementary viewpoint is to identify regions in some transform domain where the signal deviates from what we expect to find for white noise. More specifically, Flandrin proposed to identify a signal based on the distribution of the *zeros* of the short-time Fourier transform (STFT) [8]. For pure noise these zeros (as well as the distribution of local maxima) have a very regular distribution which is broken in the presence of a signal [9], [10].

This observation suggests that the important signal components can be found by identifying in the spectrogram the area of statistical deviation from the pattern expected from noise. In [11], this idea has been statistically formalized by noting that the spectrogram (for a Gaussian window) of white noise is a Gaussian entire function. For these random functions well-known statistics are available [12] that enable a statistical analysis.

G. Koliander, L. D. Abreu, A. Haimi, and J. L. Romero are with the Acoustics Research Institute, Austrian Academy of Sciences, Wohllebengasse 12–14, 1040 Vienna, Austria, email: labreau@kfs.oeaw.ac.at, ahaimi@kfs.oeaw.ac.at, guenther.koliander@oeaw.ac.at  
J. L. Romero is also with the Faculty of Mathematics, University of Vienna, Oskar-Morgenstern-Platz 1, 1090 Vienna, Austria, email: jose.luis.romero@univie.ac.at

This work was supported by the Austrian Science Fund (FWF): P 31153-N35 and P 29462-N35 and the Vienna Science and Technology Fund (WWTF): MA16-053.

We propose a scheme similar to Flandrin’s, but based on a continuous *wavelet* transform (WT) [13, Ch. 2] with analyzing wavelets of the form

$$\widehat{g}_\alpha(\xi) := \begin{cases} \xi^{\frac{\alpha-1}{2}} e^{-\xi}, & \xi \geq 0, \\ 0, & \xi < 0, \end{cases} \quad (1)$$

with  $\alpha > 1$ . The starting point of our analysis is the observation that these windows lead to WTs that map into a space of analytic functions in the upper half-plane [14]. As a consequence, we identify the point process arising from the zeros of the scalograms of white noise with the zero set of a so-called *hyperbolic Gaussian analytic function* (GAF). As in the STFT case, these GAFs have a well-understood distribution of zeros and we use this information to propose an adequate filtering procedure. More specifically, the zeros have a regular distribution with respect to the hyperbolic metric. We thus use a *hyperbolic* Delaunay triangulation of the set of zeros and proceed as in [8]: we test for a deviation on the distribution expected from white noise, by selecting significant triangles, in our case, hyperbolic triangles with unexpectedly large hyperbolic perimeter.

## II. ANALYTICITY INDUCING WAVELET TRANSFORM

Let  $g \in L^2(\mathbb{R})$  such that its Fourier transform  $\widehat{g}$  vanishes almost everywhere on  $\mathbb{R}^-$ . The continuous WT of a function (or signal)  $s \in L^2(\mathbb{R})$  with respect to the *mother wavelet*  $g \in L^2(\mathbb{R})$  is defined as

$$W_g s(x, y) = \langle s, \mathbf{T}_x \mathbf{D}_y g \rangle = \frac{1}{\sqrt{y}} \int_{\mathbb{R}} s(t) \overline{g\left(\frac{t-x}{y}\right)} dt, \quad (2)$$

for all  $x \in \mathbb{R}, y \in \mathbb{R}^+$ . Here,  $\mathbf{T}_x$  and  $\mathbf{D}_y$  denote the translation and dilation operators, respectively, given by  $(\mathbf{T}_x s)(t) = s(t-x)$ , and  $(\mathbf{D}_y s)(t) = y^{-1/2} s(t/y)$  for all  $t \in \mathbb{R}$ .

We are interested in mother wavelets  $g$  such that the image of any function is (up to scaling) an analytic function in the complex variable  $x+iy$ . The class of all  $g$  satisfying this analyticity inducing property was recently characterized in [15] and consists essentially of the Cauchy wavelets specified by (1). More specifically, the function  $x+iy \mapsto y^{-\frac{\alpha}{2}} W_{g_\alpha} s(x, y)$  is analytic for  $\alpha > 1$  and  $s \in L^2(\mathbb{R})$ . Moreover, the operator  $s \mapsto y^{-\frac{\alpha}{2}} W_{g_\alpha} s(x, y)$  is up to a constant an isometry from  $L^2(\mathbb{R})$  to the space  $A_\alpha^2 := \{f \in L^2(\Pi^+, y^{\alpha-2} dx dy) : f \text{ is analytic}\}$ , where  $\Pi^+$  denotes the upper complex halfplane [14]. The spaces  $A_\alpha^2$  are known as weighted Bergman spaces on the upper halfplane and are Hilbert spaces of analytic functions.

### III. WAVELET TRANSFORM OF WHITE NOISE

In order to analyze the properties of the WT of white noise, we first introduce a rigorous definition of white noise. Specifically, we adopt a Gaussian Hilbert space approach [16]. Let  $(\Omega, \mathcal{F}, \mathbb{P})$  be a probability space. Heuristically, one thinks of white noise on  $\mathbb{R}$  as a linear combination  $\mathcal{N} = \sum_{n=0}^{\infty} a_n e_n$  where  $a_n$  are independent standard (real or complex) Gaussians and  $\{e_n : n \geq 0\}$  is an orthonormal basis of  $L^2(\mathbb{R})$ . Unfortunately, this sum does not converge in  $L^2(\mathbb{R})$ , with probability 1. However, for any  $s \in L^2(\mathbb{R})$ , the sum

$$\mathcal{N}(s) := \sum_{n=0}^{\infty} a_n \langle e_n, s \rangle$$

converges in  $L^2(\Omega, \mathcal{F}, \mathbb{P})$  to a complex Gaussian variable with mean zero and variance  $\|s\|^2$ . A precise definition of white noise is then as the collection of random variables  $G := \{\mathcal{N}(s) : s \in L^2(\mathbb{R})\}$ . The space  $G$  is a *Gaussian Hilbert space*, that is, a Hilbert space consisting of Gaussian random variables. Its inner product is induced by  $\|\mathcal{N}(s)\|_G^2 := \|s\|^2$ . We will call the white noise real or complex depending on whether the variables  $a_n$  are real or complex standard Gaussians. The definition is independent of the choice of orthonormal basis.

We can now extend the WT with respect to the windows  $g_\alpha$  to (real or complex) white noise by

$$W_{g_\alpha}(\mathcal{N})(z) = \mathcal{N}(\mathbf{T}_x \mathbf{D}_y g_\alpha) = \sum_{n=0}^{\infty} a_n W_{g_\alpha} e_n(z), \quad (3)$$

where  $z = x + iy$ . By the isometry property of the WT, there exists a constant  $c_\alpha > 0$  such that  $\{b_n : n \geq 0\}$ , with  $b_n := c_\alpha y^{-\frac{\alpha}{2}} W_{g_\alpha}(e_n)$ , is an orthonormal basis of  $A_\alpha^2$ . The series in (3) can thus be rewritten as

$$W_{g_\alpha}(\mathcal{N})(z) = \frac{y^{\frac{\alpha}{2}}}{c_\alpha} \sum_{n=0}^{\infty} a_n b_n(z) = \frac{y^{\frac{\alpha}{2}}}{c_\alpha} f_\alpha(z), \quad (4)$$

where  $f_\alpha := \sum_{n=0}^{\infty} a_n b_n$  is a so-called hyperbolic Gaussian analytic function (GAF) [17] on  $A_\alpha^2$ . Although the GAF  $f_\alpha$  does not take values in  $A_\alpha^2$ , the defining series converges almost surely and locally uniformly to an analytic function [17]. We are interested in the distribution of zeros of the WT of white noise. By (4), we obtain that the set of zeros of  $W_{g_\alpha}(\mathcal{N})$ , where  $\mathcal{N}$  is complex white noise, has the same distribution as those of  $f_\alpha$ , the hyperbolic GAF associated with the Bergman space  $A_\alpha^2$ . This observation has recently been made simultaneously in [18] and with a slightly different definition of white noise in [19].

The zero set of GAFs is a well-studied point process. We can think of a point process as a random integer-valued measure, by setting a Dirac mass at each zero. This point process is *simple* [17, Lem. 2.4.1], which means that singletons have at most measure 1. The *first intensity function* of the zero set of  $f_\alpha$  is the function  $\rho$  satisfying

$$\mathbb{E}\#\{w \in U : f_\alpha(w) = 0\} = \int_U \rho(z) dz,$$

for every measurable subset  $U \subseteq \Pi^+$ . The first intensity of the zero set of GAFs exists and can be computed from the *Edelman-Kostlan formula* [17], [20], [21] as

$$\rho(z) = \frac{1}{4\pi y^2}. \quad (5)$$

This means that the zeros are distributed according to a multiple of the hyperbolic area density on the upper half-plane. Besides this rough description, the zeros of GAFs are known to be quite rigid: the events where the concentration of the zeros deviates significantly from what is prescribed by the first intensity are very unlikely (see, e.g., the large deviations estimates by Sodin [20] and Offord [22]). Moreover, the interaction between zeros depends only on their hyperbolic distance. Thus, we expect that the hyperbolic distance is the correct metric to assess how far zeros are away from each other in our setting. This insight is the starting point for our filtering approach based on hyperbolic triangulation.

### IV. FILTERING WITH HYPERBOLIC TRIANGULATIONS

Motivated by an idea of Flandrin [8], we expect that the distribution of zeros in the scalogram can be used to identify important signal components. More specifically, due to the interaction between zeros for the WT of white noise, there is a quite rigid distribution of these zeros in parts that are dominated by noise and a signal might interfere with this distribution and enable us to identify signal parts.

To identify the zero set, we use that the wavelet transformed signal is analytic and, thus, local minima of the modulus must be zeros. In the discrete scalogram, we declare a point a zero if it is smaller than its 4 neighbors. Experimentally, the number of zeros found by this procedure fits well the expected number of zeros prescribed by the one-point intensity function (5).

Similar to the method proposed in [8], we consider a triangulation of the zero set. However, as the interaction between zeros is not governed by Euclidean distance but by hyperbolic distance, we consider a hyperbolic triangulation of the zero set. To this end, we use the fact that the edges constructed by a Euclidean triangulation are a superset of the edges of the hyperbolic triangulation [23]. We can even find the triangles that belong to the Euclidean but not to the hyperbolic triangulation by calculating the circumcircle related to each triangle. Only if such a circle is contained in the upper halfplane, the associated triangle is also part of the hyperbolic triangulation [23].

The hyperbolic distance between the points  $(x_1, y_1)$  and  $(x_2, y_2)$  is given by

$$d_h\left(\begin{pmatrix} x_1 \\ y_1 \end{pmatrix}, \begin{pmatrix} x_2 \\ y_2 \end{pmatrix}\right) = 2 \sinh^{-1} \left( \frac{\left\| \begin{pmatrix} x_1 \\ y_1 \end{pmatrix} - \begin{pmatrix} x_2 \\ y_2 \end{pmatrix} \right\|}{2\sqrt{y_1 y_2}} \right).$$

The shortest connection between two points is along a geodesic, which are in this setting halfcircles centered on the  $x$ -axis or vertical lines  $x = \text{const}$ . In particular, a hyperbolic triangulation is best illustrated using these geodesics to connect the points. An illustration is given in Fig. 1. Following the reasoning in [8], we expect that for pure noise

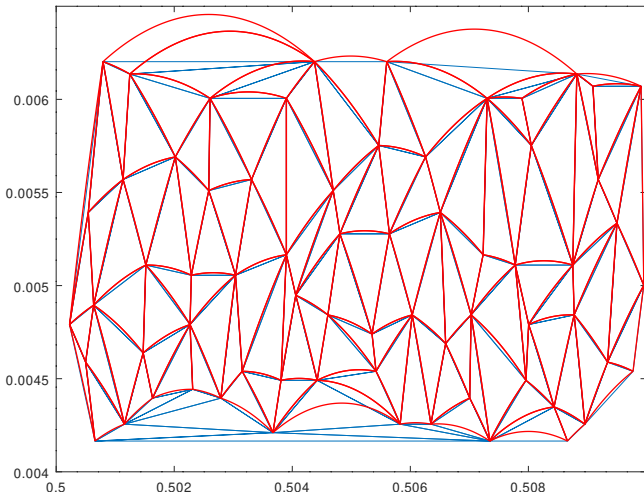


Fig. 1. Euclidean (blue) and hyperbolic (red) triangulation of the same point pattern. Note that not all triangles in the Euclidean triangulation do also belong to the hyperbolic triangulation.

the triangles in a hyperbolic Delaunay triangulation will all have approximately the same hyperbolic perimeter. If the perimeter differs significantly from the one observed for noise, we consider the area of the hyperbolic triangle to be part of the signal. Unfortunately, deriving a closed form expression of the expected hyperbolic perimeter  $p_h$  is beyond the scope of this work, but based on a large number of simulations, we observed that  $p_h \approx 12.1/\sqrt{\alpha}$  for a pure noise signal and a wide range of  $\alpha$  (50 to 10 000). The choice of a threshold  $\tau$  above which a triangle is considered to contain signal components is of course a tradeoff between interpreting noise as signal and missing signal components. We take a very strict choice of  $\tau = 17/\sqrt{\alpha}$  which a pure noise triangle exceeds experimentally only with probability  $6 \cdot 10^{-4}$ . Because signal components usually span more than a single triangle, we disregard triangles that do not share at least one corner with another triangle above the threshold. This reduces the observed probability that a noise triangle is wrongly considered a signal component to below  $10^{-4}$ . Finally, to avoid the most significant boundary effects, we also exclude all triangles that have a corner point on the boundary of the considered region.

## V. EXPERIMENTS

We performed some preliminary experiments of the proposed method to illustrate the strength and weaknesses. The signals we consider are taken from the EBU SQAM database [24] and white noise with the same average power as the signal is added. We use the WT with mother wavelet  $g_\alpha$  and interpret the unique peak of  $g_\alpha$  in the frequency domain as the frequency associated with a given scale (cf. [15, Sec. IV]).

The first example is the violin signal 8 in [24] from 0.4s to 2.4s. Fig. 2 shows the scalogram and masked scalogram for  $\alpha$  and illustrates that not all the high energy components are found by the proposed method. In particular, well resolved components can by chance have exactly the width that results in triangles that have the same perimeter as pure noise triangles. Even reducing the threshold  $\tau$  did not recover more

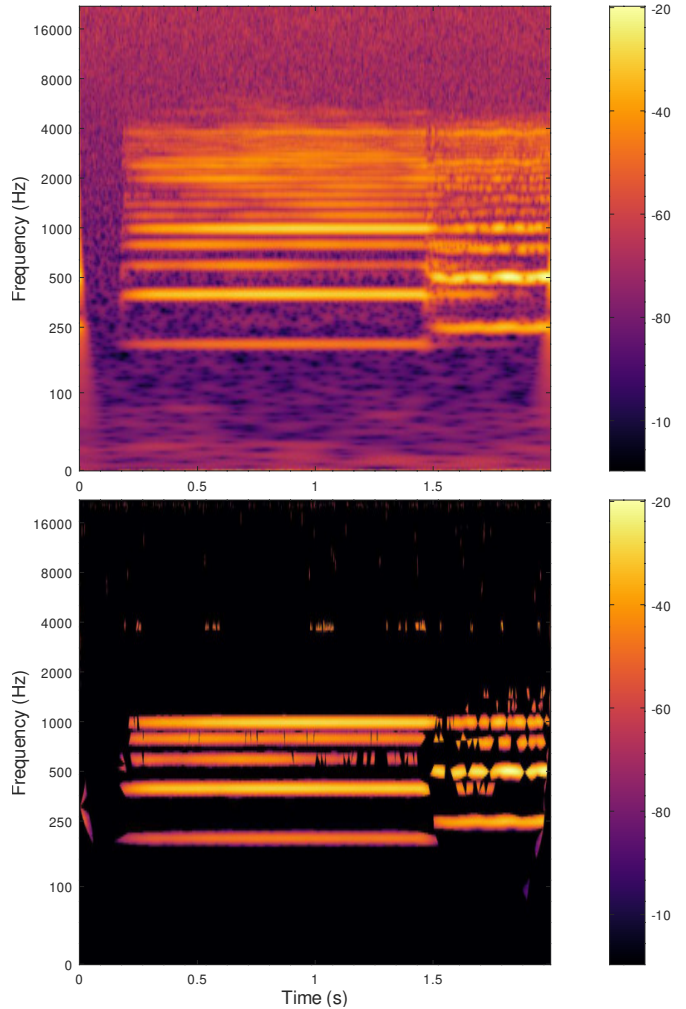


Fig. 2. Scalogram of a two second violin signal in white noise (top) and masked scalogram based on hyperbolic triangulation (bottom).

signal components but mainly increased noise. This is to be expected as the theory only provides understanding of what properties we expect from pure noise components but does not exclude the possibility that also specific signal parts may share these properties. Due to this problem it is reasonable to set the threshold high as in this case the identified components are with high probability signal components. We also considered other values of  $\alpha$  and observed that higher values more easily detect higher frequency components whereas boundary effects are more pronounced and low frequency components are not as well identified.

The second example we considered is the male English voice signal 50 in [24] from 0.4s to 2.4s. In Fig. 3, we show the scalogram and masked scalogram for the setting  $\alpha = 300$  and observe that the mask is quite patchy. In the lower frequency components the mask follows the signal components reasonably well although some smaller triangles are missed. Again, we observed for higher  $\alpha$  a better identification of higher frequency components and vice versa. In particular, more triangles are missed for greater  $\alpha$  and it is difficult to see the structure of the signal in the masked scalogram.

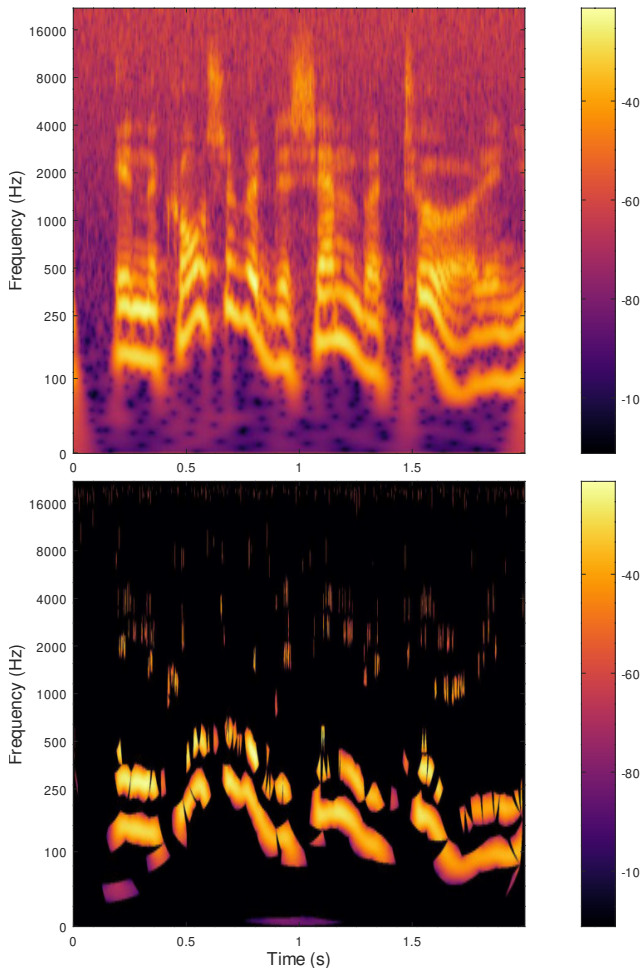


Fig. 3. Scalogram of a two second male voice signal in white noise (top) and masked scalogram based on hyperbolic triangulation (bottom).

## VI. CONCLUSION

We presented an approach to generalize a method proposed in [8] to WTs. Using analyticity inducing wavelets, we used the relation to GAFs to obtain a basic understanding of the distribution of the zero pattern of the wavelet transformed signal. This relation allowed us to identify the hyperbolic metric as the natural distance between zeros. Translating the triangulation idea to this setting, we analyzed some preliminary signals and found that we can identify some but not all signal components.

Many questions regarding optimal choices of parameters and thresholds can be considered in future work. For example, the exact role of the parameter  $\alpha$  is largely unknown and so far we only observed in limited experiments that high-frequency components are better identified by larger  $\alpha$ . Furthermore, the threshold chosen for the detection of signal components is at the moment only based on experimental results for pure noise signals. A more detailed analysis of the expected hyperbolic distance between points and its variance for the hyperbolic GAF would allow for a better founded choice. Finally, the method does not by itself allow for a reliable denoising or identification of signals. Since the method primarily finds larger signal regions but does not at all rely on the magnitude

of signal components, a combination with established thresholding techniques seems promising.

## REFERENCES

- [1] D. L. Donoho and I. M. Johnstone, "Ideal spatial adaptation by wavelet shrinkage," *Biometrika*, vol. 81, no. 3, pp. 425–455, Sep. 1994.
- [2] G. Yu, S. Mallat, and E. Bacry, "Audio denoising by time-frequency block thresholding," *IEEE Trans. Signal Process.*, vol. 56, no. 5, pp. 1830–1839, May 2008.
- [3] I. Daubechies and S. Maes, "A nonlinear squeezing of the continuous wavelet transform based on auditory nerve models," in *Wavelets in Medicine and Biology*, A. Aldroubi and M. Unser, Eds. Boca Raton, FL: CRC Press, 1996, pp. 527–546.
- [4] F. Auger and P. Flandrin, "Improving the readability of time-frequency and time-scale representations by the reassignment method," *IEEE Trans. Signal Process.*, vol. 43, no. 5, pp. 1068–1089, May 1995.
- [5] F. Auger, P. Flandrin, Y.-T. Lin, S. McLaughlin, S. Meignen, T. Oberlin, and H.-T. Wu, "Time-frequency reassignment and synchrosqueezing: An overview," *IEEE Signal Process. Mag.*, vol. 30, no. 6, pp. 32–41, Nov. 2013.
- [6] R. A. Carmona, W. L. Hwang, and B. Torresani, "Characterization of signals by the ridges of their wavelet transforms," *IEEE Trans. Signal Process.*, vol. 45, no. 10, pp. 2586–2590, Oct. 1997.
- [7] N. Delprat, B. Escudié, P. Guillemain, R. Kronland-Martinet, P. Tchamitchian, and B. Torresani, "Asymptotic wavelet and Gabor analysis: Extraction of instantaneous frequencies," *IEEE Trans. Inf. Theory*, vol. 38, no. 2, pp. 644–664, Mar. 1992.
- [8] P. Flandrin, "Time-frequency filtering based on spectrogram zeros," *IEEE Signal Process. Lett.*, vol. 22, no. 11, pp. 2137–2141, 2015.
- [9] —, "On spectrogram local maxima," in *Proc. IEEE Int. Conf. Acoust. Speech Signal Process.*, New Orleans, LA, Mar. 2017, pp. 3979–3983.
- [10] —, "The sound of silence: Recovering signals from time-frequency zeros," in *Proc. Asilomar Conf. Signals Syst. Comput.*, Pacific Grove, CA, Nov. 2016.
- [11] R. Bardenet, J. Flamant, and P. Chainais, "On the zeros of the spectrogram of white noise," *Appl. Comput. Harmon. Anal.*, 2019, in press.
- [12] N. D. Feldheim, "Zeros of Gaussian analytic functions with translation-invariant distribution," *Israel J. Math.*, vol. 195, no. 1, pp. 317–345, 2013.
- [13] I. Daubechies, *Ten Lectures on Wavelets*. SIAM, 1992.
- [14] I. Daubechies and T. Paul, "Time-frequency localisation operators—a geometric phase space approach: II. The use of dilations," *Inverse Prob.*, vol. 4, no. 3, pp. 661–680, Aug. 1988.
- [15] N. Holighaus, G. Koliander, Z. Průša, and L. D. Abreu, "Characterization of analytic wavelet transforms and a new phaseless reconstruction algorithm," *submitted to IEEE Trans. Sig. Process.*, 2018. [Online]. Available: <http://tftat.github.io/notes/tftatnote053.pdf>
- [16] S. Janson, *Gaussian Hilbert spaces*, ser. Cambridge Tracts in Mathematics. Cambridge University Press, Cambridge, 1997, vol. 129.
- [17] J. B. Hough, M. Krishnapur, Y. Peres, and B. Virág, *Zeros of Gaussian analytic functions and determinantal point processes*, ser. University Lecture Series. Providence, RI: Amer. Math. Soc., 2009, vol. 51.
- [18] L. D. Abreu, A. Haimi, G. Koliander, and J. L. Romero, "Filtering with wavelet zeros and Gaussian analytic functions," *arXiv preprint:1807.03183*, 2018. [Online]. Available: <https://arxiv.org/abs/1807.03183v2>
- [19] R. Bardenet and A. Hardy, "Time-frequency transforms of white noises and Gaussian analytic functions," *arXiv preprint:1807.11554*, 2018. [Online]. Available: <https://arxiv.org/pdf/1807.11554.pdf>
- [20] M. Sodin, "Zeros of Gaussian analytic functions," *Math. Res. Lett.*, vol. 7, no. 4, pp. 371–381, 2000.
- [21] A. Edelman and E. Kostlan, "How many zeros of a random polynomial are real?" *Bulletin of the American Mathematical Society*, vol. 32, no. 1, pp. 1–37, 1995.
- [22] A. C. Offord, "The distribution of zeros of power series whose coefficients are independent random variables," *Indian J. Math.*, vol. 9, pp. 175–196, 1967.
- [23] J.-D. Boissonnat, A. Cerezo, O. Devillers, and M. Teillaud, "Output sensitive construction of the 3D Delaunay triangulation of constrained sets of points," *Int. J. Comput. Geometry Appl.*, vol. 6, no. 1, pp. 1–14, 1996.
- [24] "Tech 3253: Sound Quality Assessment Material recordings for subjective tests," Eur. Broadc. Union, Geneva, Tech. Rep., Sept. 2008.